2023.10.17 Journal Club

Benchmark between CDCC and Faddeev method

Phys. Rev. C **76**, 064602 (2007)
Phys. Rev. C **85**, 054621 (2012)
Phys. Rev. C **94**, 051603 (2016)

Junzhe Liu

$d + ^{12}C$ elastic scattering

1, good overall agreement

2, Faddeev and CDCC can not reproduce backward angles data

3, coupling is important

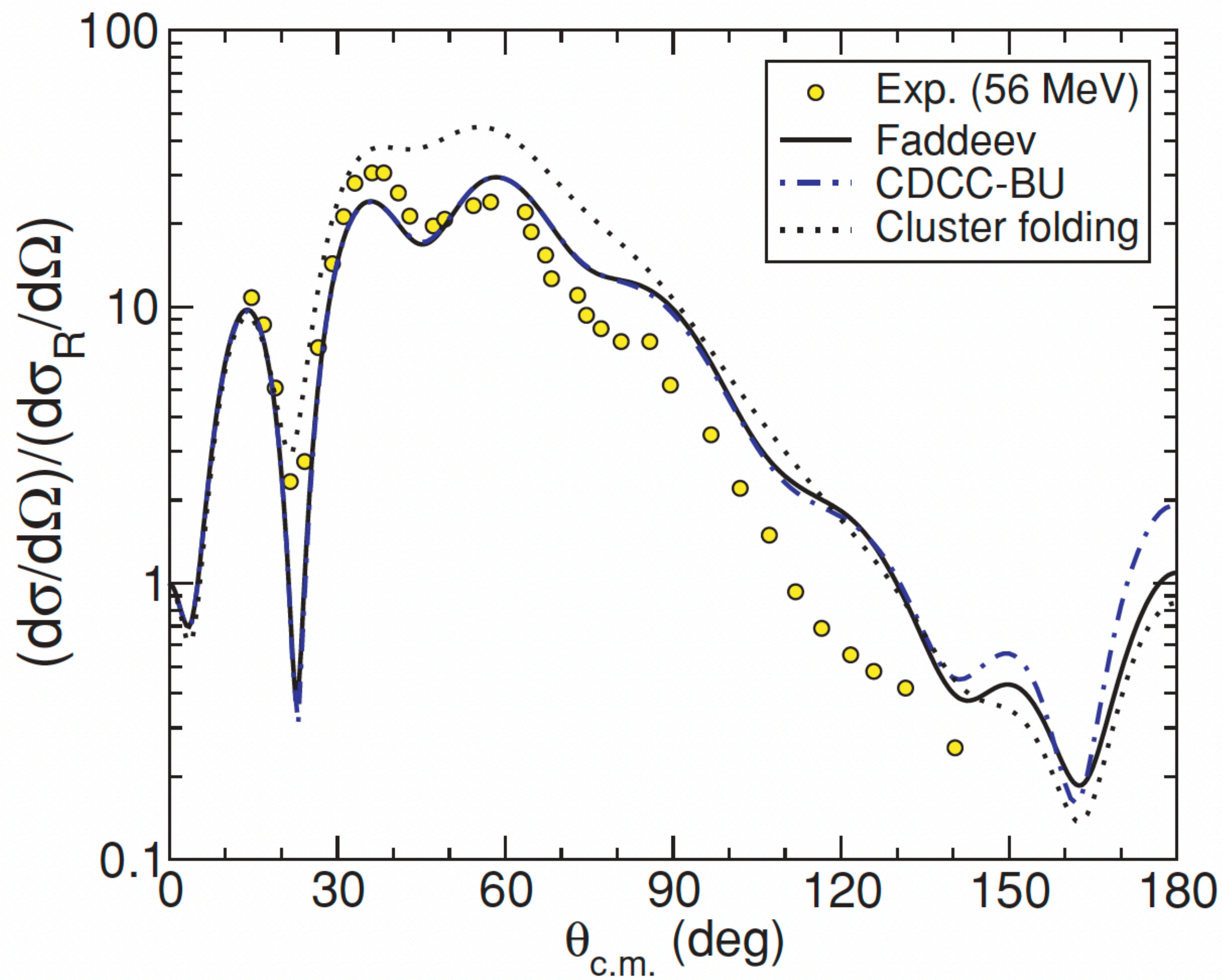

FIG. 2. (Color online) Elastic cross section for deuterons on ^{12}C at $E_d = 56$ MeV: the solid line corresponds to exact three-body results and the dash-dotted line to CDCC. The result of a single channel cluster folding (dotted) is also shown. The experimental data are from Ref. [22].

$d + ^{12}C$ elastic scattering

1, good overall agreement

2, Coulomb interaction

Can not be neglected

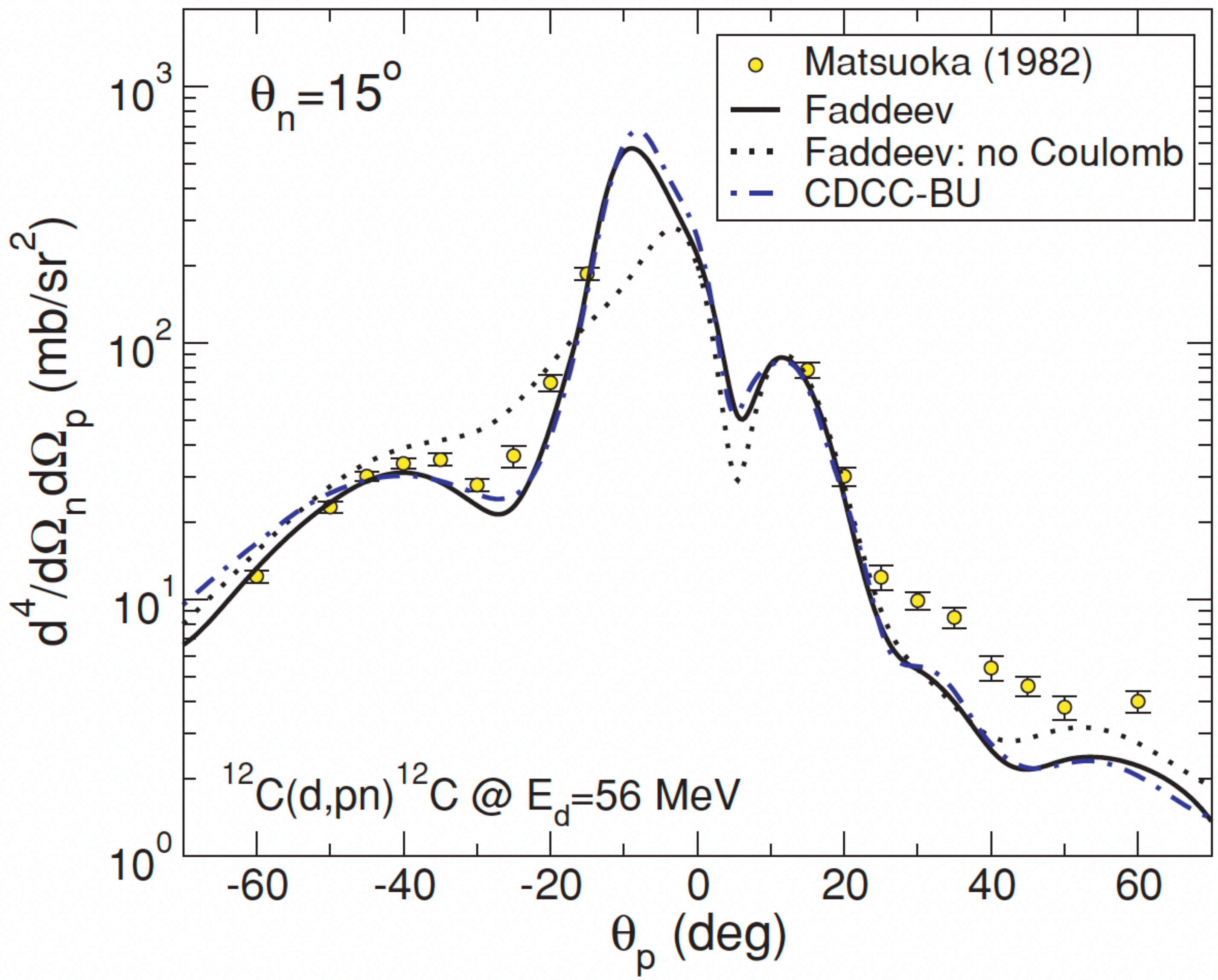

FIG. 3. (Color online) Semi-inclusive differential cross section vs proton scattering angle for the breakup of deuterons on ^{12}C at $E_d = 56$ MeV: the solid line corresponds to the exact three-body results and the dash-dotted line to CDCC. The dotted line corresponds to the three-body exact result in the absence of the Coulomb force. The experimental data are from Ref. [36].

$^{12}C(d,pn)$ breakup

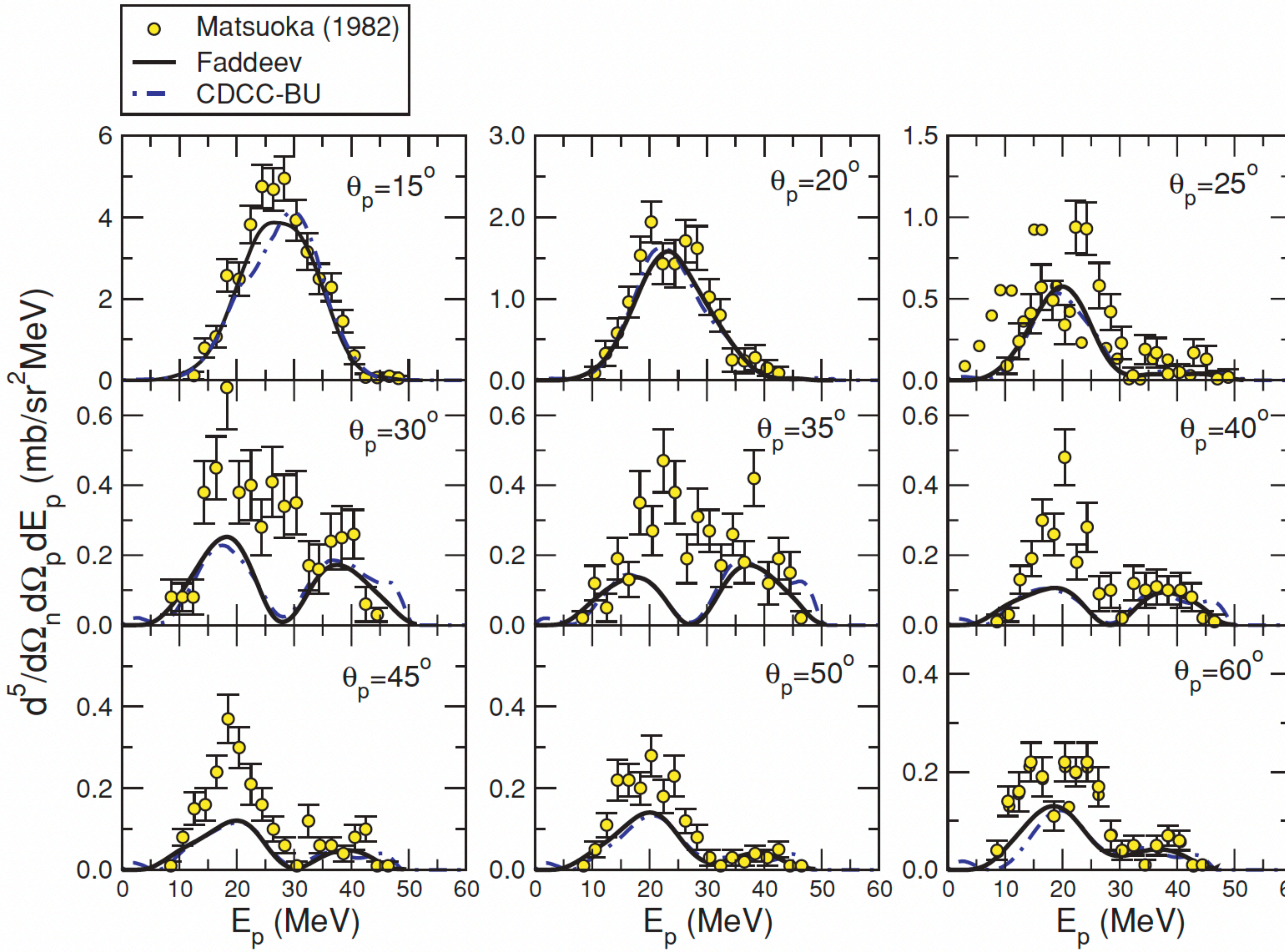

FIG. 4. (Color online) Exclusive differential cross section vs proton energy for the breakup of deuterons on ^{12}C at $E_d = 56$ MeV, $\theta_n = 15°$, and $\theta_p > 0$: the solid line corresponds to exact three-body results and the dash-dotted line to CDCC. The experimental data are from Ref. [36].

$^{12}C(d, pn)$ breakup

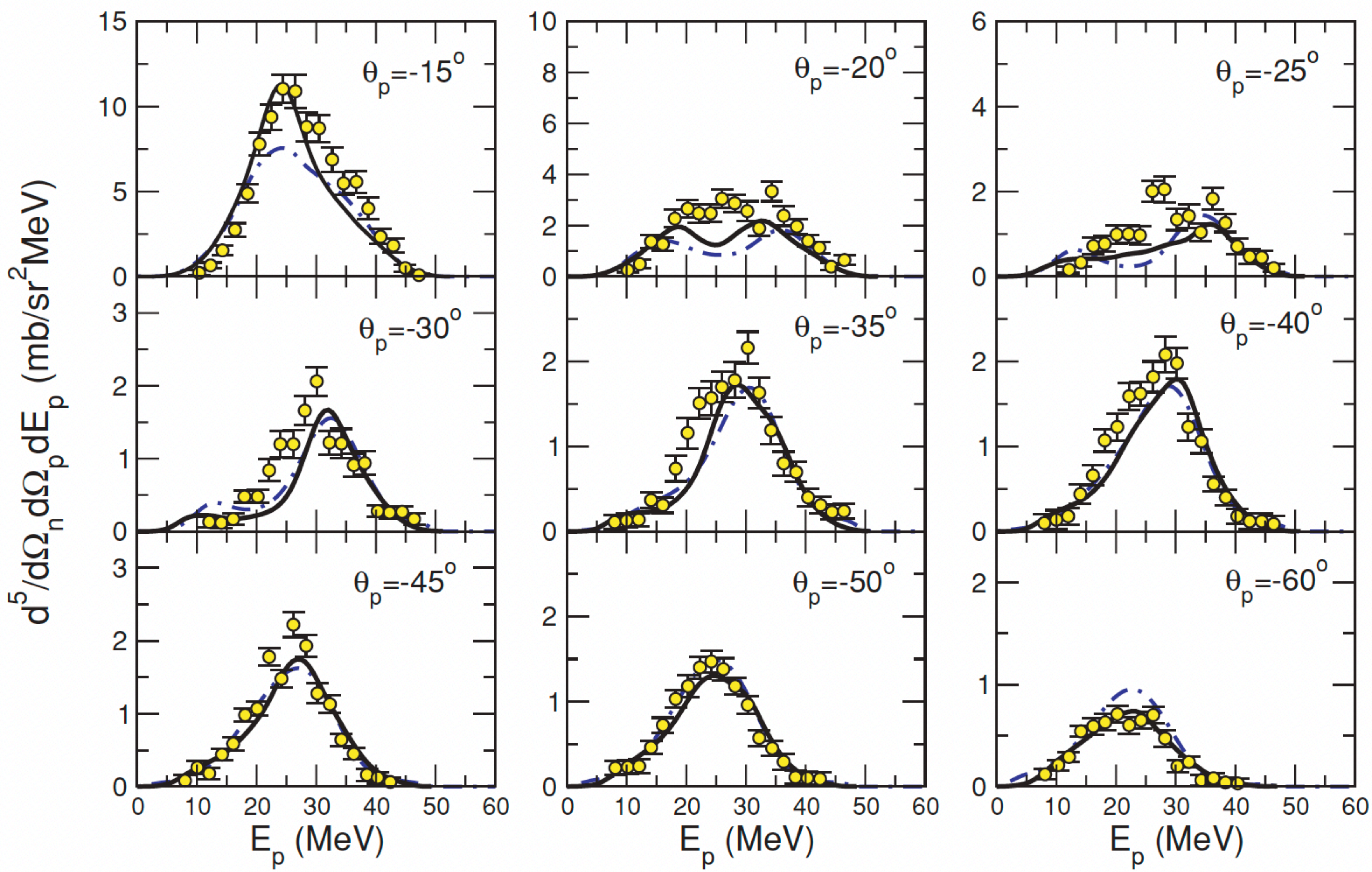

$d + ^{58}$Ni elastic scattering

1， good overall agreement

2， Coupling effect is important

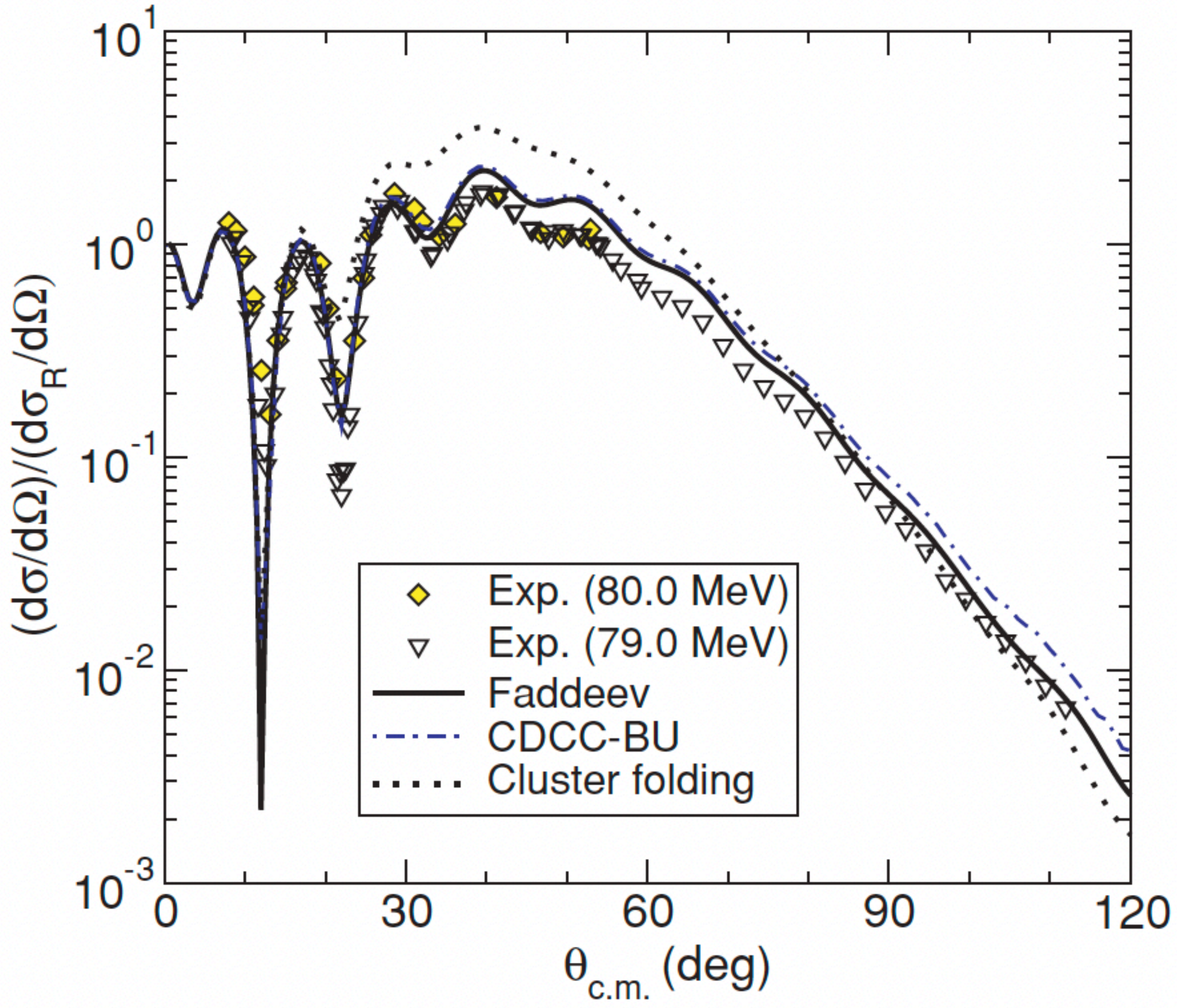

FIG. 6. (Color online) Elastic cross section for deuterons on ^{58}Ni at $E_d = 80$ MeV: the solid line corresponds to the exact three-body results and the dash-dotted line to CDCC results. The experimental data at 80 MeV (diamonds) are from Ref. [23], and those at 79 MeV (triangles) are from Ref. [24]. The dotted line is the CDCC calculation suppressing the coupling to the deuteron continuum (see text).

$p + ^{11}$Be elastic scattering

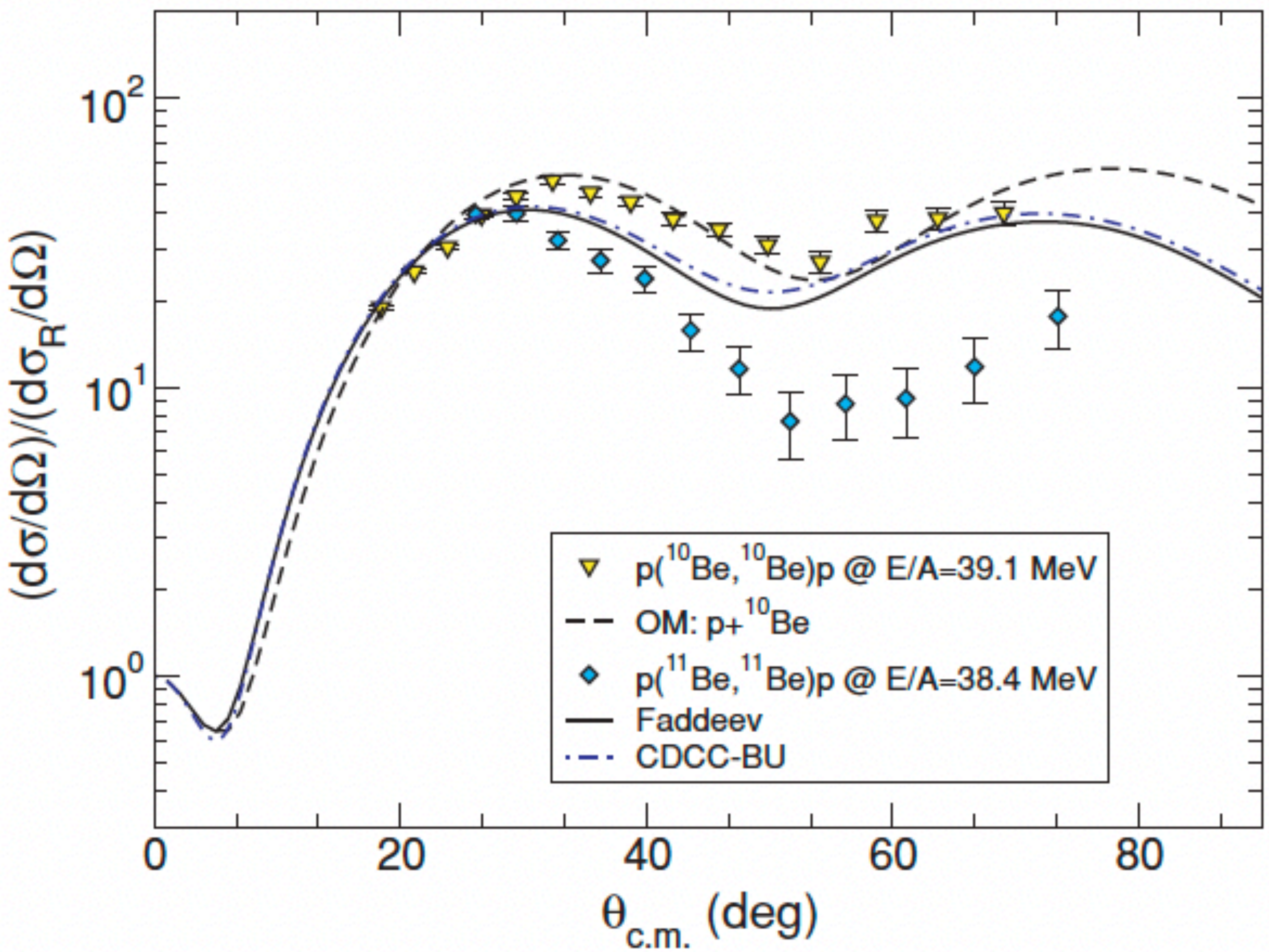

FIG. 7. (Color online) ^{1}H(^{11}Be, ^{11}Be)p elastic cross section at $E_{\mathrm{Lab}}/A = 38.4$ MeV. The solid line corresponds to exact three-body results while the dash-dotted line to CDCC. The dashed line corresponds to an optical potential fit to the corresponding ^{10}Be-p data of Ref. [25] shown by the triangles. The diamonds correspond to ^{11}Be-p elastic data of Ref. [25].

$p(^{11}\mathrm{Be},^{10}\mathrm{Be})d$ **transfer reaction**

CDCC-TR* $T_{\mathrm{prior}} = \langle \Psi_f^{(-)} | U_{xt} + U_{ct} - U_{pt} | \phi_p \chi_p \rangle$

Disagreement may

Indicate that here

CDCC method can

Not reproduce the

3B wave function

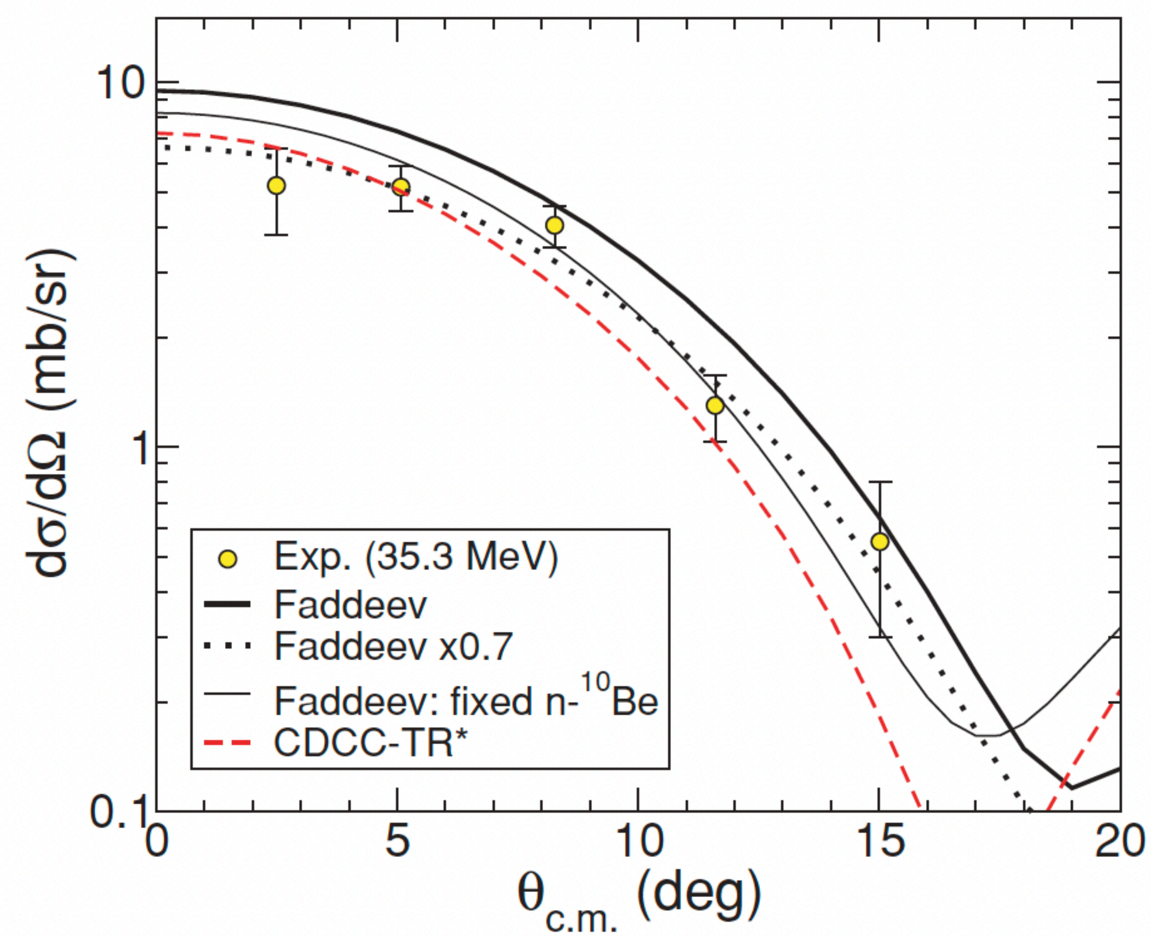

FIG. 8. (Color online) Transfer reaction $^1\mathrm{H}(^{11}\mathrm{Be},\,^{10}\mathrm{Be})d$ cross section at $E_{\mathrm{Lab}}/A = 38.4$ MeV. The thick solid line corresponds to the exact three-body result, while the dotted line corresponds to the same calculation multiplied by 0.7. The thin solid line is the exact calculation with a partial-wave independent n-^{10}Be interaction. The latter is to be compared with the CDCC-TR* calculation (dashed line), as explained in the text. The experimental data are from Ref. [39] at $E_p = 35.3$ MeV.

$p(^{11}\mathrm{Be},^{10}\mathrm{Be})pn$ breakup reaction

1， CDCC is not well converged

2， CDCC can only Reproduce the Shape

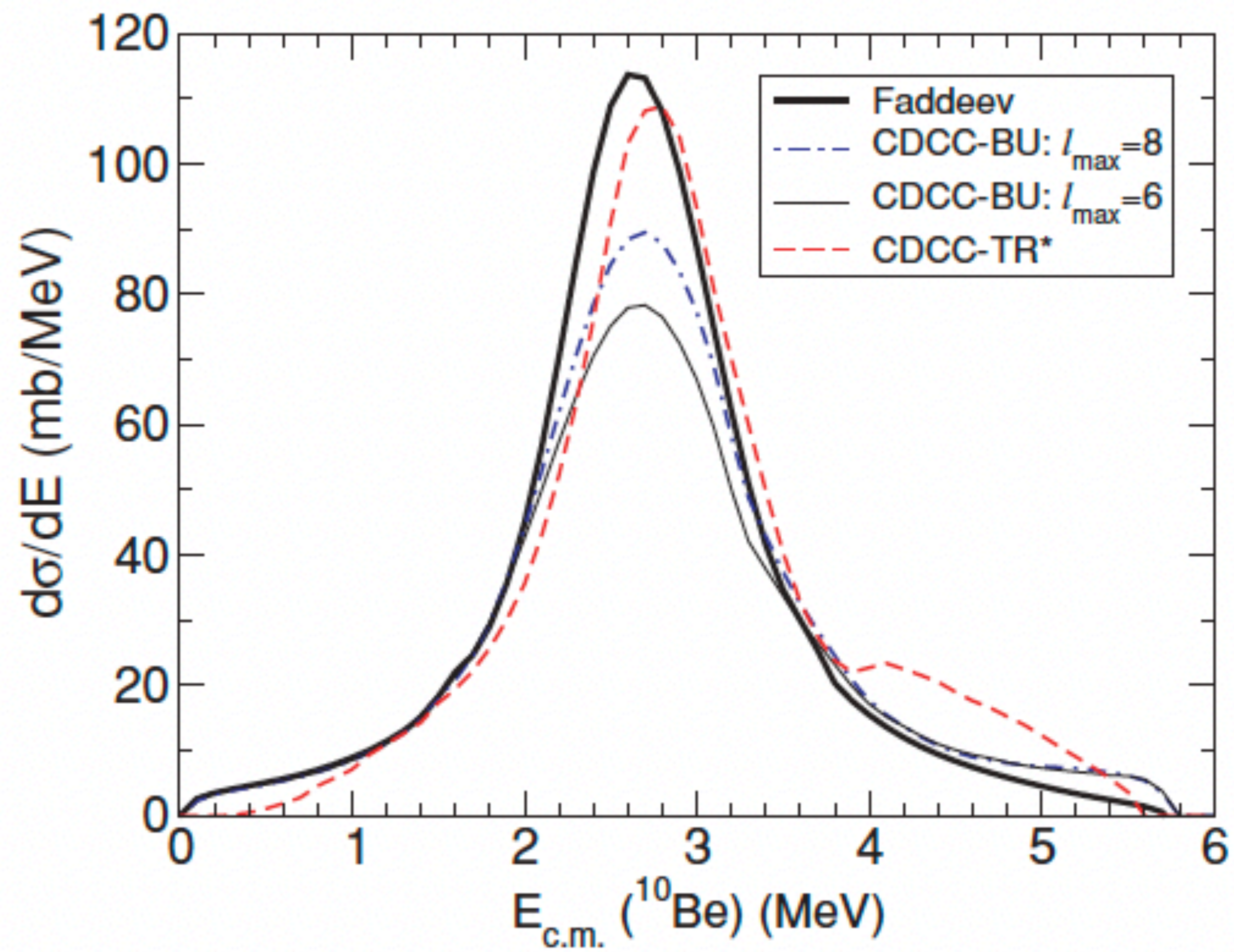

FIG. 9. (Color online) Semi-inclusive differential cross section for the reaction $^{1}\mathrm{H}(^{11}\mathrm{Be},^{10}\mathrm{Be})pn$, at $E_{\mathrm{Lab}}/A = 38.4$ MeV, vs ^{10}Be center of mass energy. The thick solid line corresponds to exact three-body results, the dashed line to CDCC-TR*, the dash-dotted line and the thin solid line to CDCC-BU with $l_{\mathrm{max}} = 8$ and $l_{\mathrm{max}} = 6$, respectively.

$p + ^{11}$Be elastic scattering

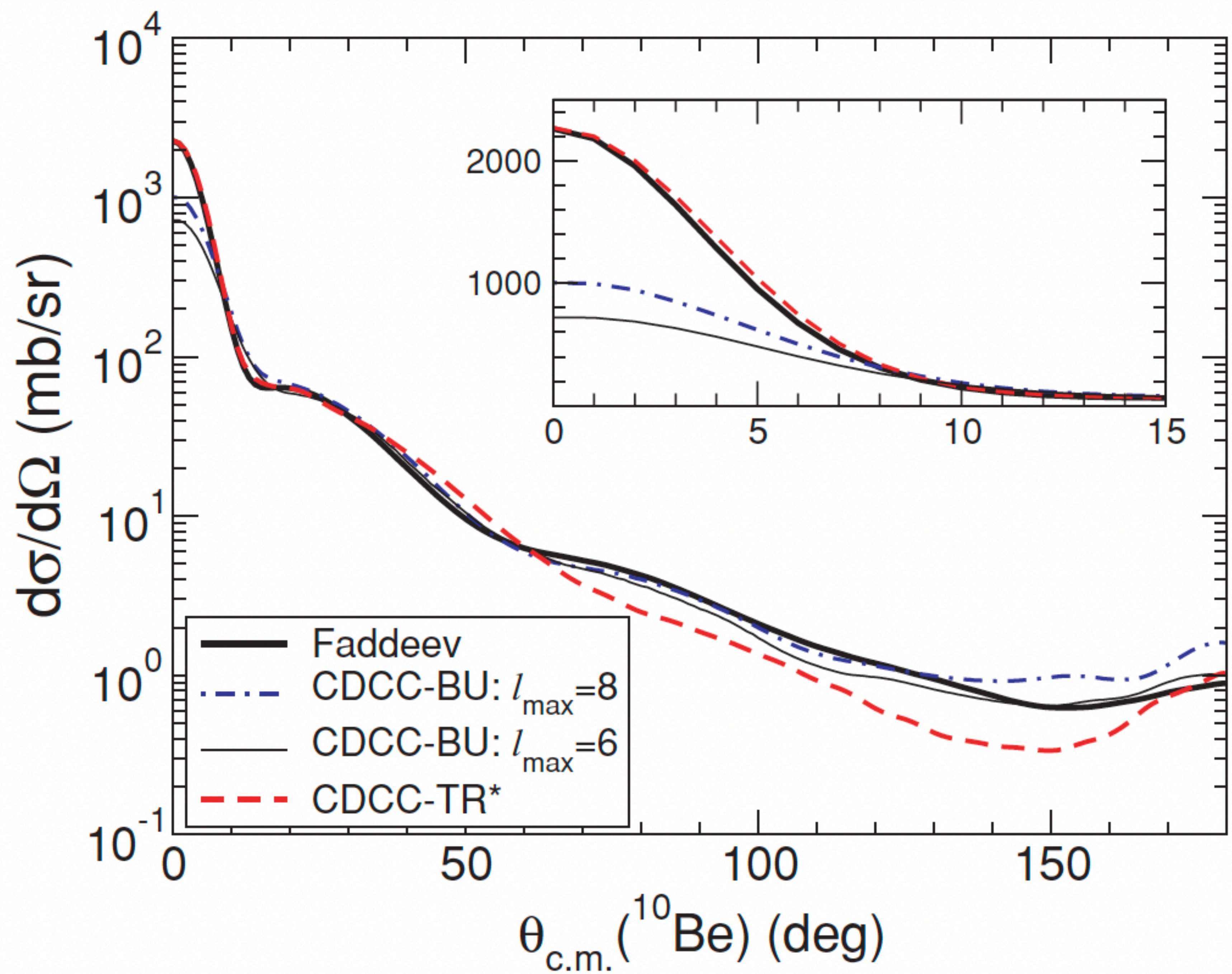

FIG. 10. (Color online) Same as Fig. 9, but showing ^{10}Be angular distribution after energy integration.

elastic scattering involving deuteron

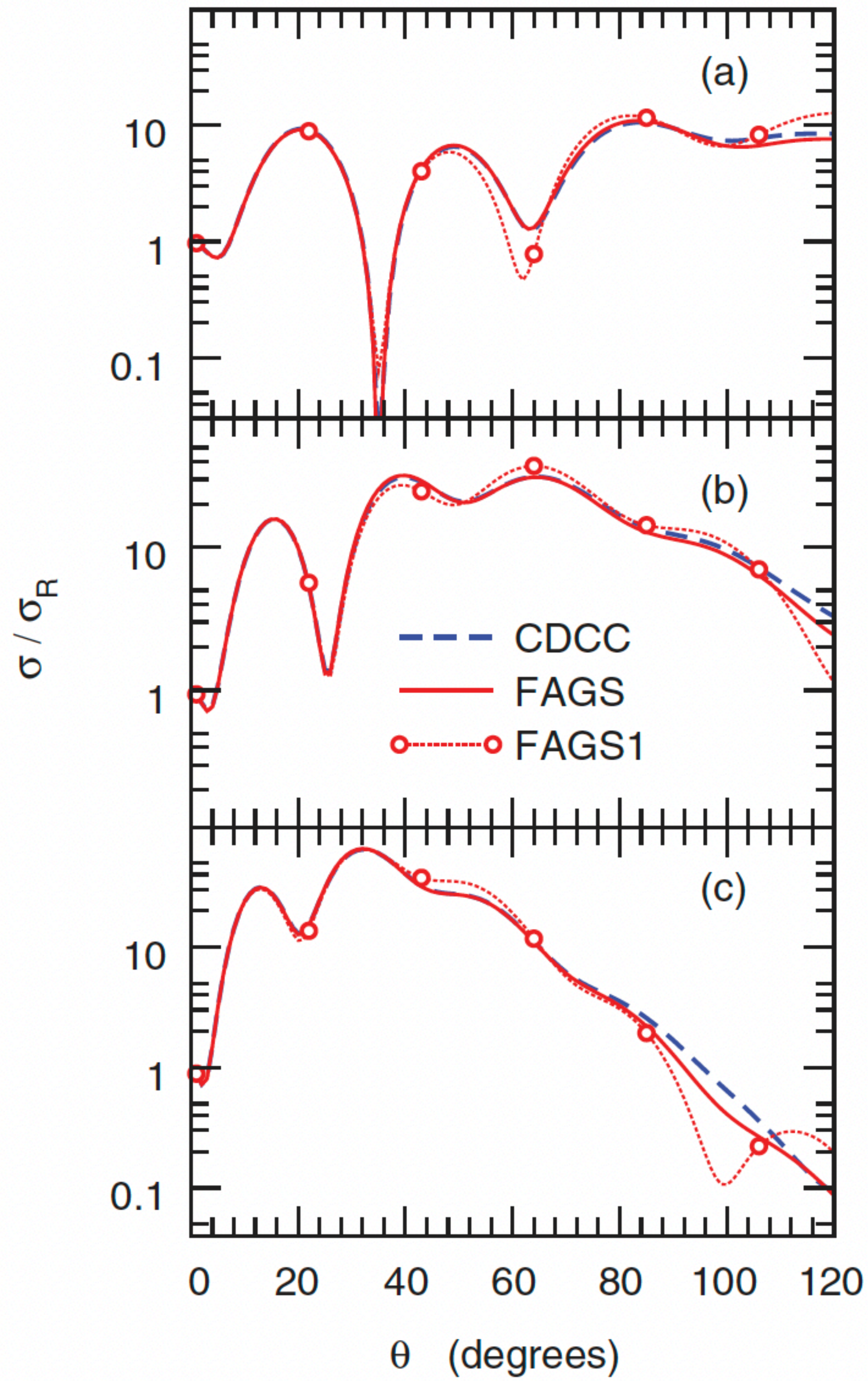

FIG. 2. (Color online) Elastic cross section for $d+^{10}\mathrm{Be}$: (a) $E_\mathrm{d} = 21.4$ MeV, (b) $E_\mathrm{d} = 40.9$ MeV, and (c) $E_\mathrm{d} = 71$ MeV.

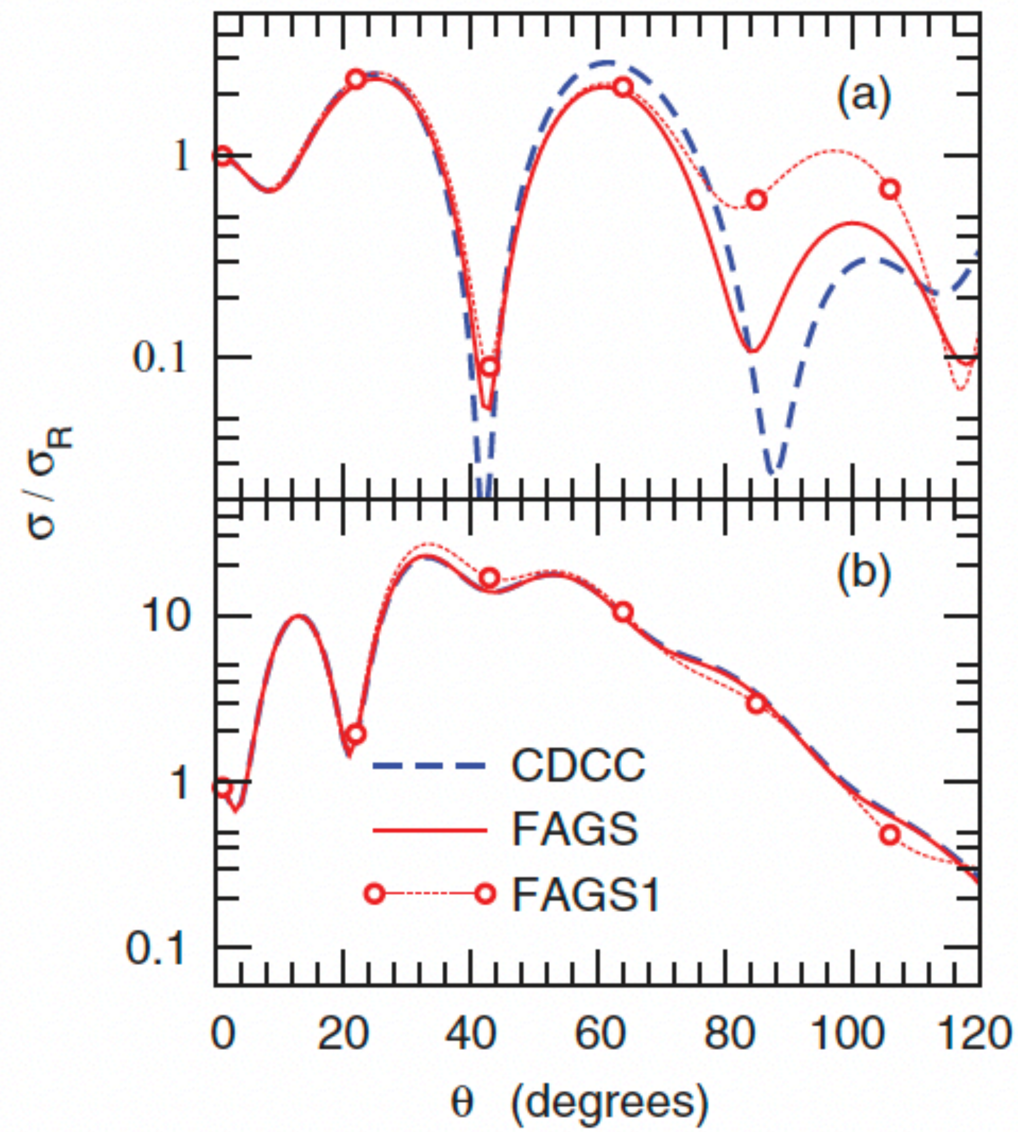

FIG. 3. (Color online) Elastic cross section for $d+^{12}\mathrm{C}$: (a) $E_\mathrm{d} = 12$ MeV and (b) $E_\mathrm{d} = 56$ MeV.

elastic scattering involving deuteron

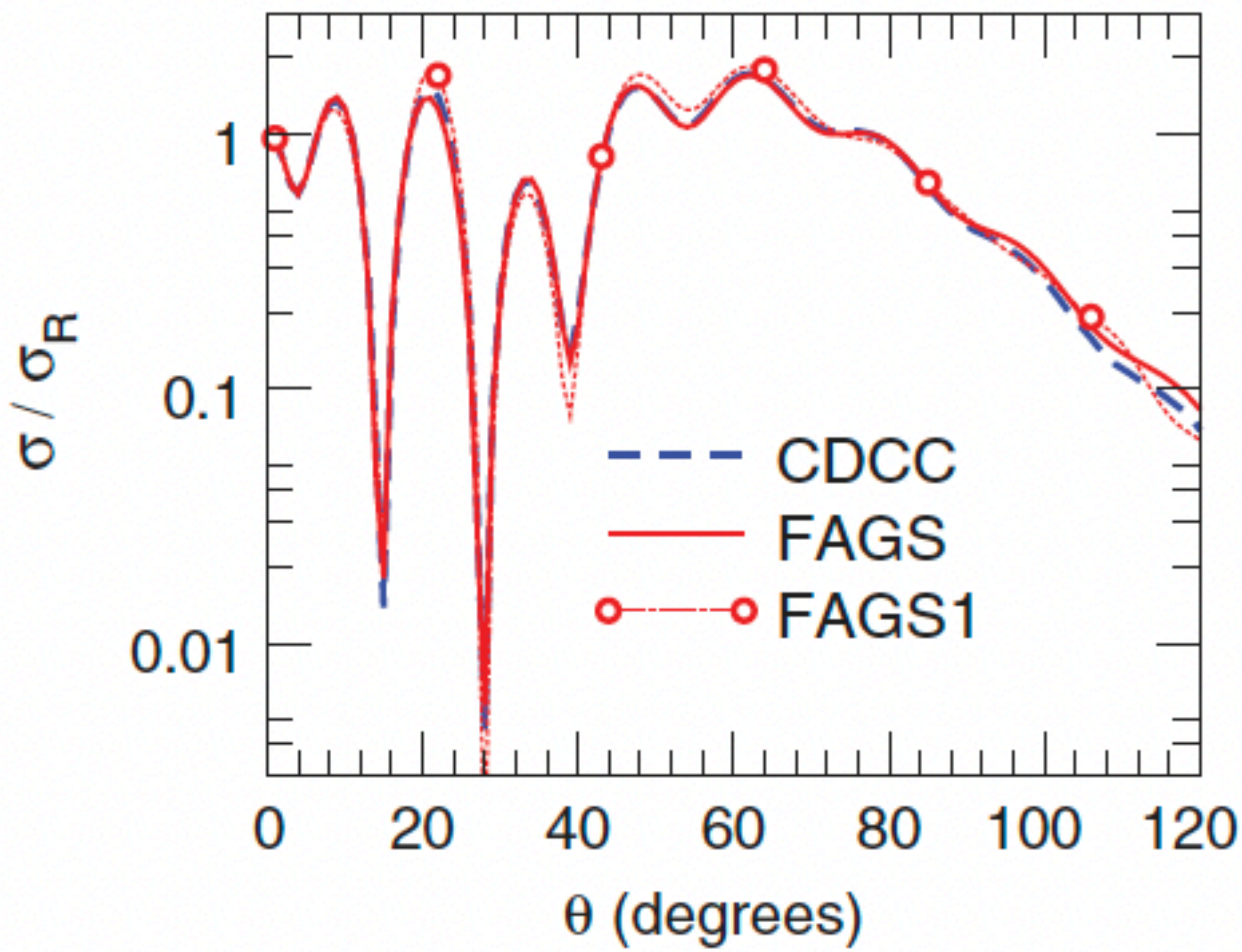

FIG. 4. (Color online) Elastic cross section for $d+^{48}Ca$ at $E_d = 56$ MeV.

transfer scattering

Significant discrepancies
Appear at higher energy

Two sets of auxiliary
potential are included
To test how much of
The discrepancy can be
Attributed to the choice of
Optical potential

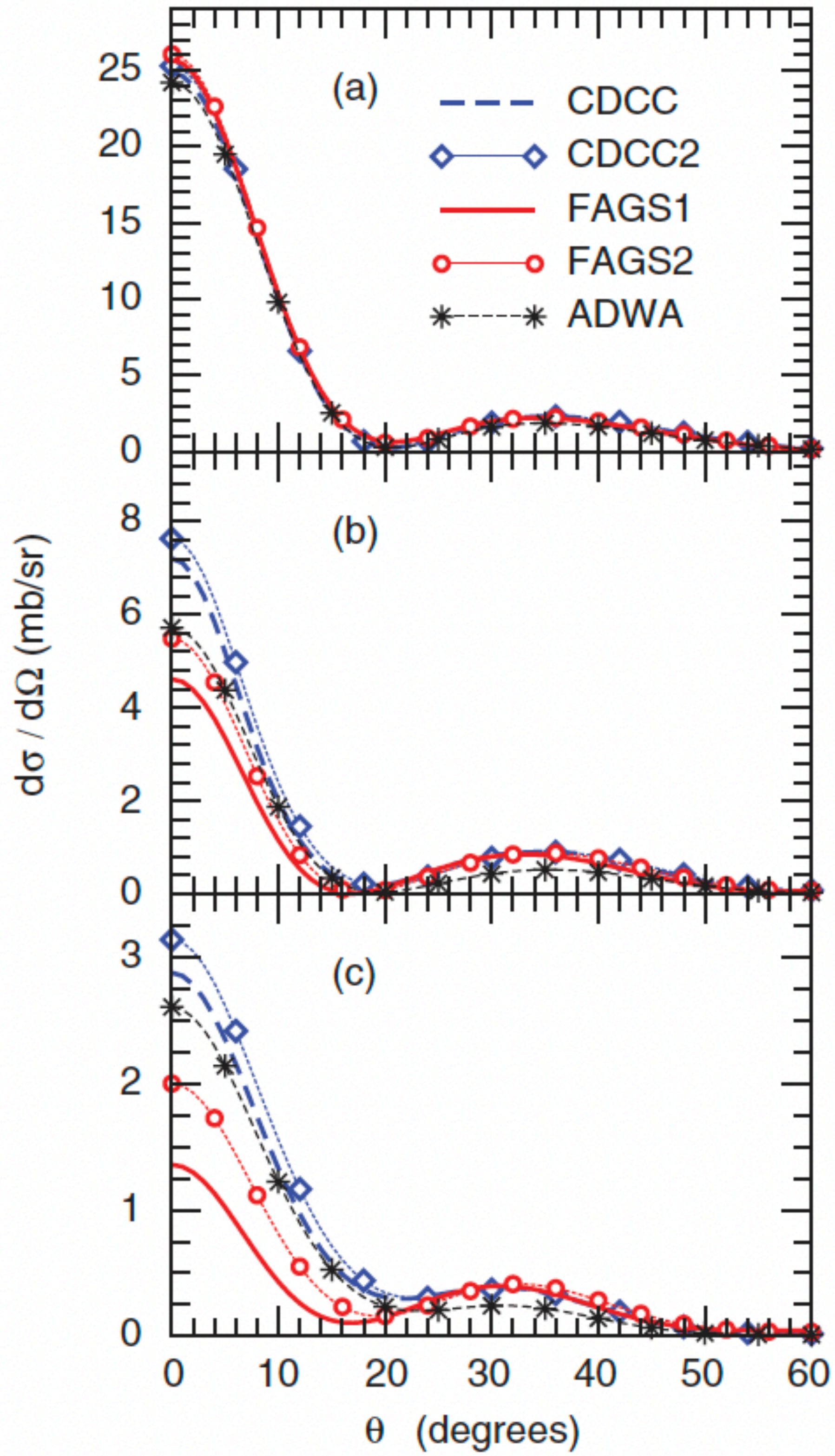

FIG. 5. (Color online) Angular distribution for ^{10}Be(d, p)^{11}Be: (a) $E_d = 21.4$ MeV, (b) $E_d = 40.9$ MeV, and (c) $E_d = 71$ MeV.

transfer scattering

Significant discrepancies
Appear at higher energy

No dependency of
The selection of
The optical potential

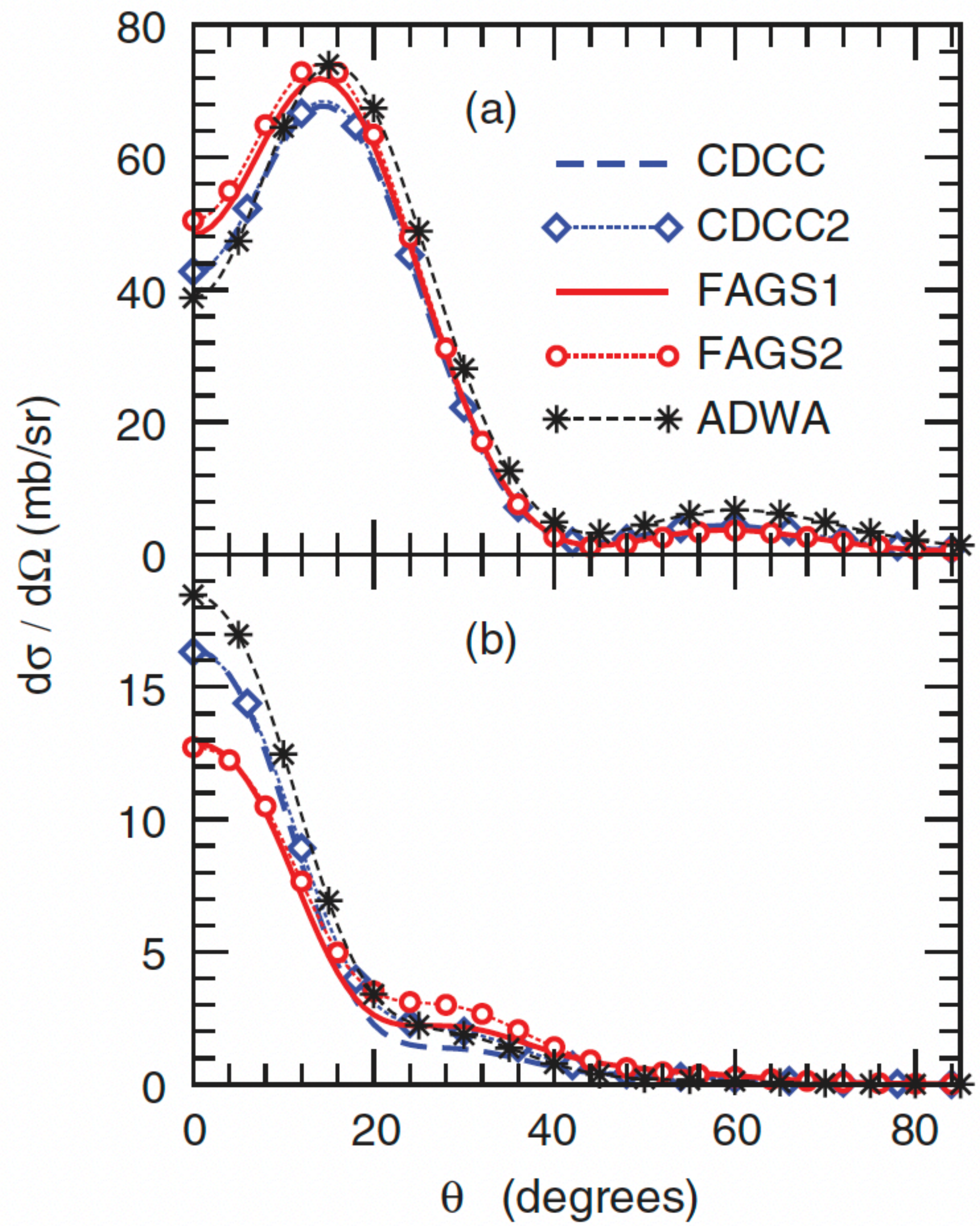

FIG. 6. (Color online) Angular distribution for $^{12}C(d, p)^{13}C$: (a) $E_d = 12$ MeV and (b) $E_d = 56$ MeV.

transfer scattering

Discrepancies between
Optical potentials
And Faddeev/CDCC

Hard to make conclusion

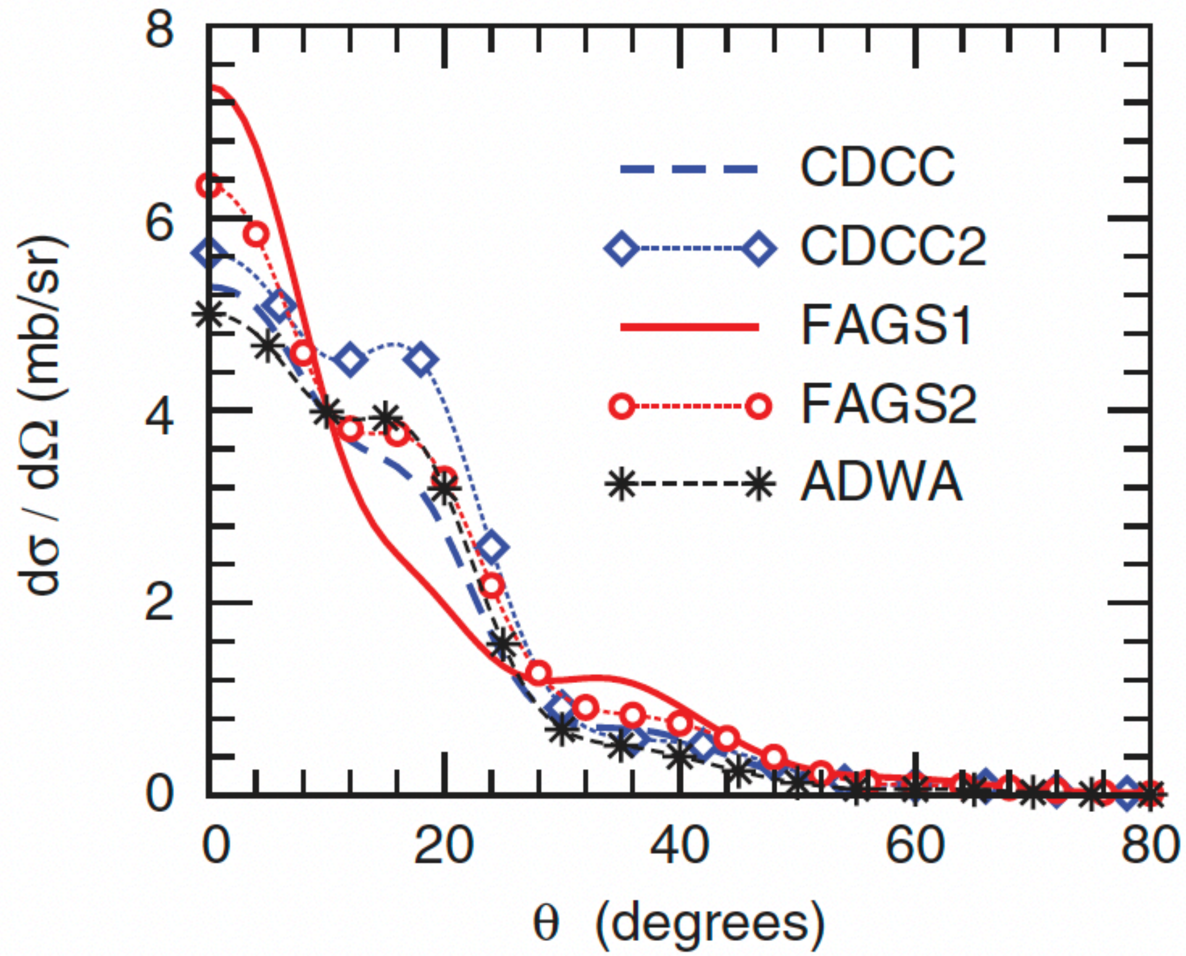

FIG. 7. (Color online) Angular distribution for $^{48}Ca(d, p)^{49}Ca$ at $E_d = 56$ MeV.

deuteron breakup

Significant discrepancies
Appears
Even taking into
Account the error estimated
With model space truncation

This discrepancy
Is removed when
Energy goes up

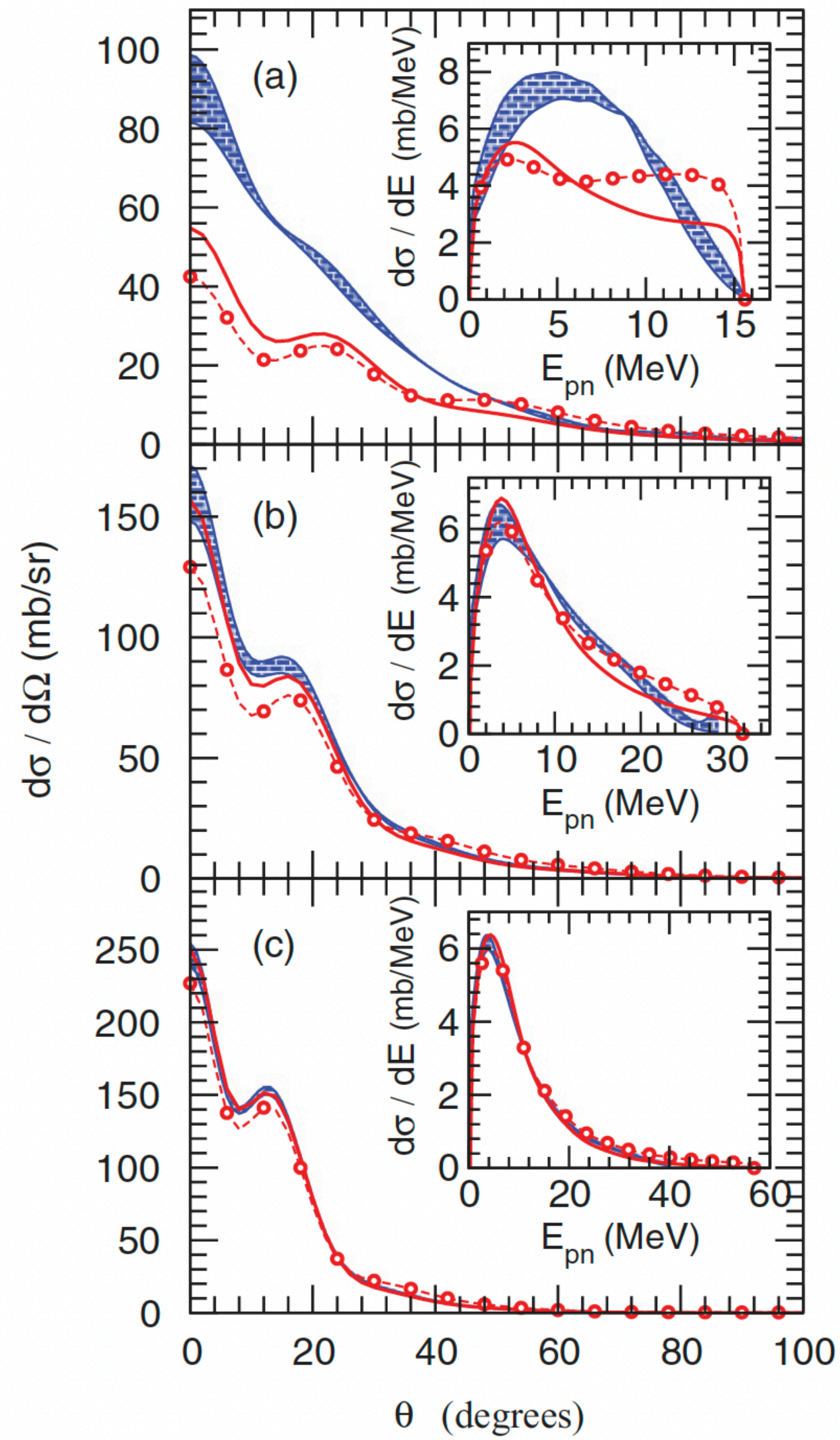

FIG. 8. (Color online) Breakup distributions for the $^{10}Be(d, pn)^{10}Be$ reaction at (a) $E_d = 21$ MeV, (b) $E_d = 40.9$ MeV, and (c) $E_d = 71$ MeV. Results for CDCC (hatched band), FAGS (solid), and FAGS1 (circles).

deuteron breakup

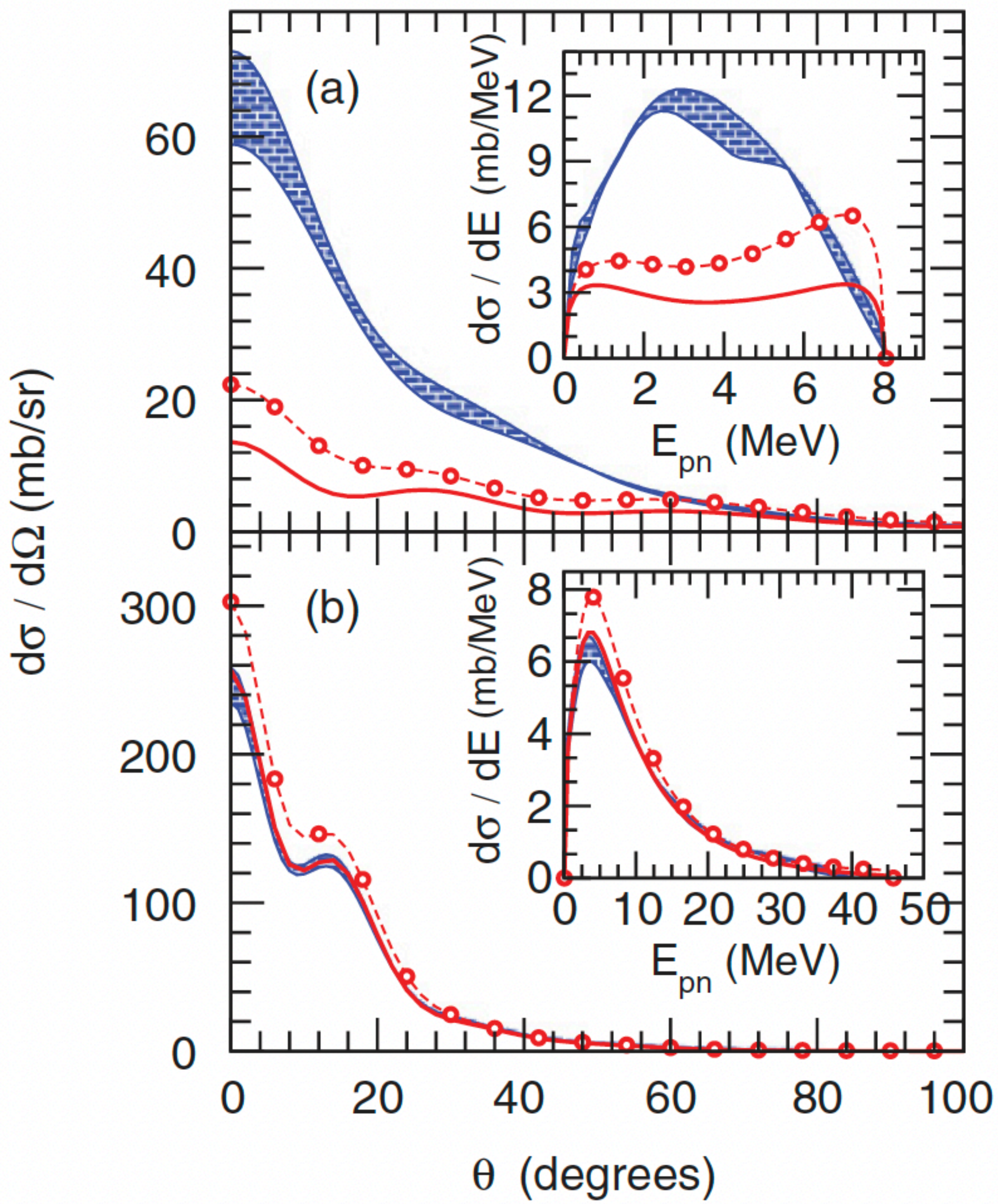

FIG. 9. (Color online) Breakup distributions for the $^{12}C(d, pn)^{12}C$ reaction at (a) $E_d = 12$ MeV and (b) $E_d = 56$ MeV. Results for CDCC (hatched band), FAGS (solid), and FAGS1 (circles).

deuteron breakup

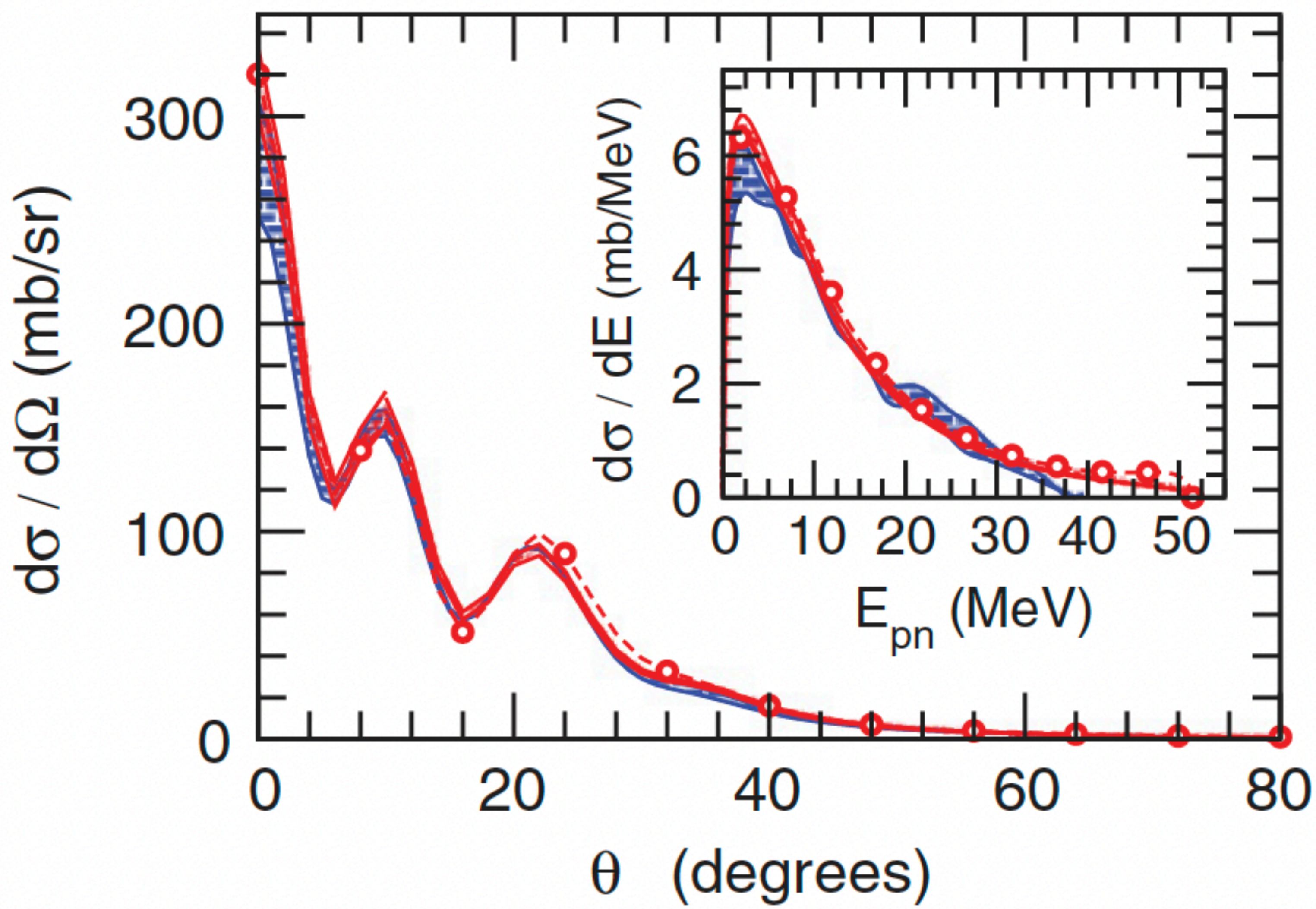

FIG. 10. (Color online) Breakup distributions for the ^{48}Ca(d, pn)^{48}Ca reaction at $E_d = 56$ MeV. Results for CDCC (hatched band), FAGS (solid), and FAGS1 (circles).

closed channel

open channel $$\chi_c \to U^{(-)}_{L,\eta_i}\left(K_i R\right)\delta_{cc_0} - \sqrt{K_0/K_i}S_{cc_0}U^{(+)}_{L,\eta_i}\left(K_i R\right)$$

closed channel $$\chi_c \to -S_{cc_0}W_{-\eta_i,L+1/2}\left(-2iK_i R\right)$$

For closed channels $S-$matrix is not related to observables directly.

closed channel

All channel： converged and match well

only open channel： significant discrepancy

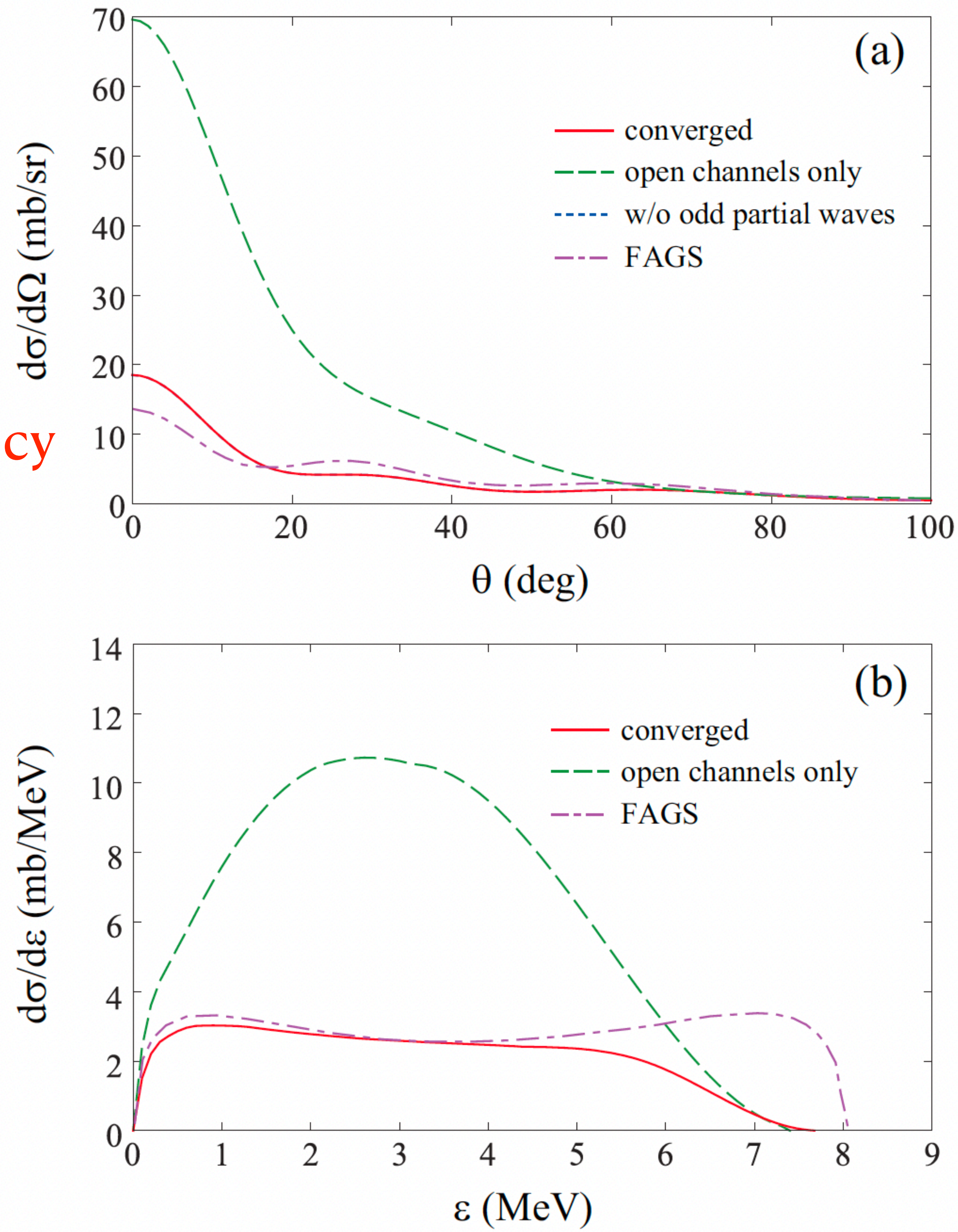

FIG. 1. (a) Angular distribution and (b) breakup energy distribution of the elastic breakup cross section for $^{12}\mathrm{C}\,(d,pn)^{12}\mathrm{C}$ at $E_d = 12\,\mathrm{MeV}$. The solid, dashed, and dash-dotted lines in each panel show the converged CDCC result, the result of the CDCC method calculated with including only the open channels, and the result of FAGS theory taken from Ref. [11], respectively. The dotted line in (a) is the same as the solid line but omitting the odd partial waves between p and n.

closed channel

Same calculation but for $^{10}Be(d,pn)^{10}Be$ @ 21MeV

Well converged when
Including all channels

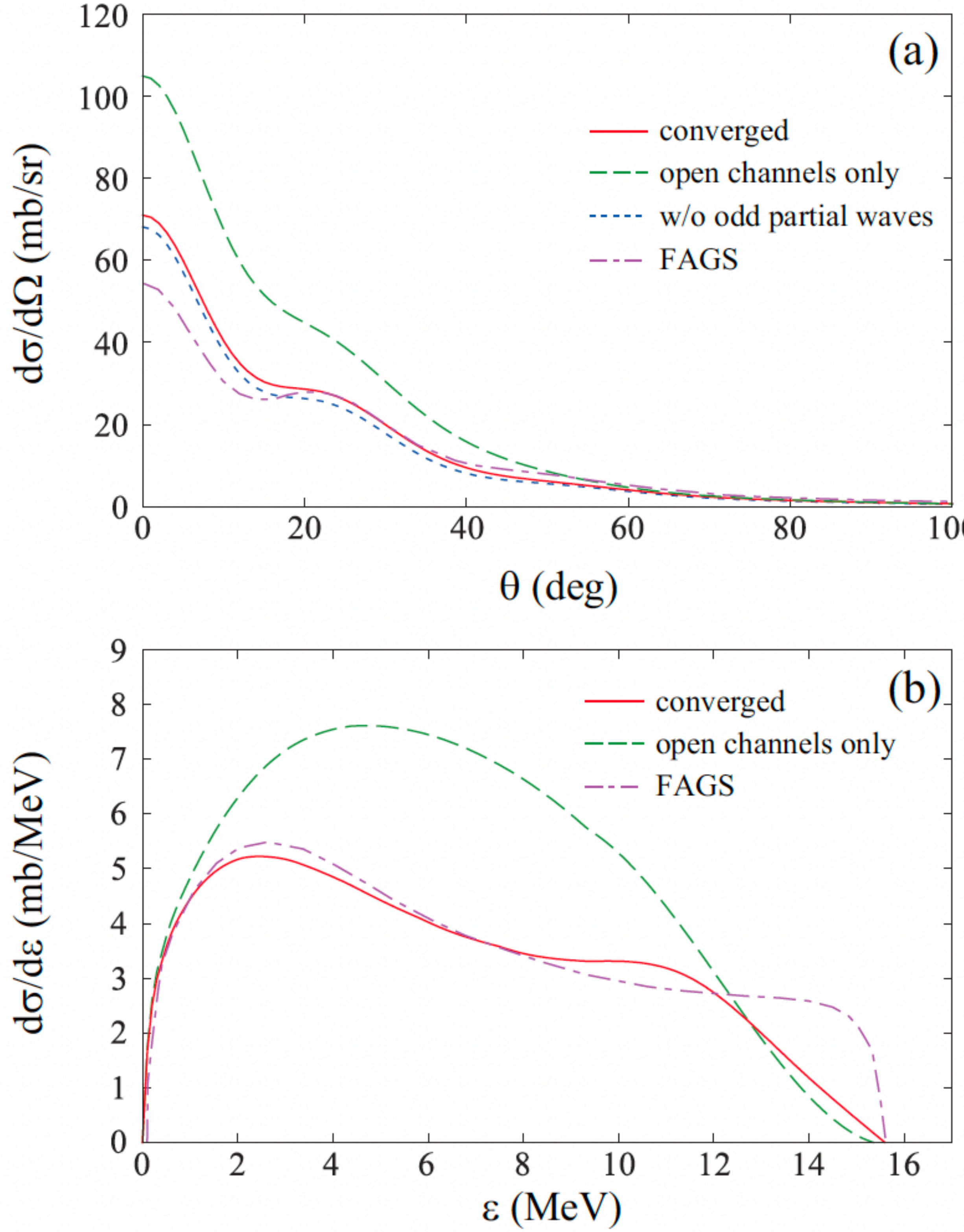

FIG. 3. Same as Fig. 1 but for $^{10}Be\,(d,pn)^{10}Be$ at $E_d = 21$ MeV.

Summary

1. CDCC is able to provide a good approximation to FAGS for elastic scattering.
2. CDCC is a very good approximation of FAGS at reactions around 10 MeV/u, but not so good for higher beam energies.
3. Significant discrepancy occurs when evaluating break up reactions. But when energy goes higher, CDCC reproduces the FAGS results well.
4. Inclusion of closed channels may solve the above problem.